MEASUREMENT OF SURFACE RESISTANCE PROPERTIES WITH COAXIAL RESONATORS – REVIEW*

HyeKyoung Park[1, 2 †], S. U. De Silva[1], J. R. Delayen[1]
[1]Center for Accelerator Science, Old Dominion University, Norfolk, VA 23529, USA
[2]Thomas Jefferson National Accelerator Facility, Newport News, VA 23606, USA

Abstract

Achieving ever decreasing surface resistance at higher field in superconducting RF accelerating structures is one of the most outstanding developments in modern accelerators. The BCS theory [1] has been used widely to estimate the surface resistance and to guide the technology. However, recent research results show that the behaviour of the surface resistance further deviates from the BCS theory [2]. So far, the study on surface resistance was performed usually with cavities of single frequency which limited the study of frequency dependent surface resistance. The Center for Accelerator Science at Old Dominion University has designed and built several half-wave coaxial cavities (HWR) to study the frequency, temperature, and RF field dependence of surface resistance of superconductor [3]. TRIUMF in Canada also joined this line of research using such multi frequency quarter wave (QWR) and half-wave coaxial cavities [4, 5]. This type of multi- mode cavity will allow us to systematically study the parameters affecting surface resistance on the same surface. In this paper, we review the results ODU and TRIUMF collected so far and present proper analysis methods.

MULTI-MODE CAVITIES

Historic Note

The frequency dependence study of R_s and R_{res} using half wave coaxial was done by L. Szécsi in 1970 [6]. He used a lead-coated half-wave coaxial cavity and tested the frequency dependence of the surface resistance. He measured the surface resistance of superconducting lead from 375 MHz to 5 GHz and reported in his paper that the frequency dependence of $R_{BCS} \sim \omega^{1.83}$ and $R_{res} \sim \omega^{1.78}$.

Cavity Design

The advantage of a coaxial cavity is that the surface field is concentrated on the center conductor and the distribution is almost identical for all TEM modes. Therefore, we can study the same surface for the all TEM frequencies. ODU's half-wave coaxial cavity was designed to provide a range of frequencies of particular interest and separate TEM modes from neighbouring TE or TM modes. It was also designed to achieve high rf surface field in the center conductor and be free of multipacting [3]. TRIUMF designed and fabricated both HWR and QWR (217 and 648

MHz). The modes and their design frequencies are listed in the Table 1.

Table 1: Mode and Frequency of Half-Wave Cavities

Mode	Frequency [MHz] ODU HWR	Frequency [MHz] TRIUMF HWR
TEM1	325	389
TEM2	651	778
TEM3	976	1166
TEM4	1301	1555

Material was carefully selected to be compatible with future surface treatment. Figure 1 shows the completed cavities.

Figure 1: HWR and QWR of TRIUMF and HWR of ODU. Bottom picture is the center conductor subassembly before welding the outer conductor of ODU HWR.

STUDY METHODOLOGY

Cavity Preparation

Cavity preparation followed a typical recipe. The listed steps below are used for ODU half-wave coaxial cavity. TRIUMF's QWR was prepared with almost identical steps but with different duration of the 800 C heat treatment 6 hours and the 120 C bake for 48 hours.

- Bulk BCP – 200 microns.
- Heat treatment – at 800 C for 3 hours. See Fig. 2 for the furnace temperature profile and the residual gas trace.

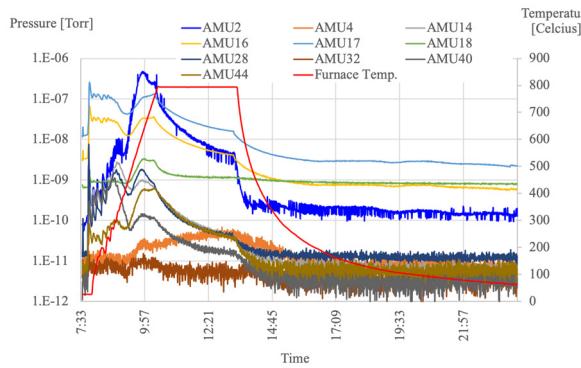Fundamental R&D - Nb

field-dependence

Figure 2: 800 C heat treatment of ODU HWR.

- Light BCP – 20 microns.
- High pressure rinse – ODU HWR has 4 ports on each end cap. Rinsing wand went through the 2 ports.
- Cleanroom assembly – Cavity was assembled with a power input coupler, a pick up coupler, vacuum valve, and burst disc. Both couplers are fixed loop couplers.
- Instrumentation – Before the cavity was loaded in a dewar, temperature sensors and magnetic field probes are installed on the cavity.
- Baseline test
- Low temperature (120 C) bake for 6 hours – Cavity was baked in the bake box where the control thermocouple was attached in the center of the outer conductor (see Fig. 3). Cavity was actively pumped during the baking. During the baking, the partial pressure of residual gas was monitored. The trace of the elements is shown in Fig. 4.

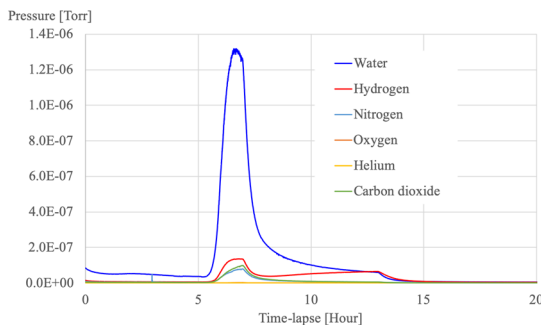Figure 3: ODU HWR with thermocouples installed in the bake box.

Figure 4: RGA monitoring of half wave coaxial cavity during 120 C bake.

- Test – Cavity was loaded (see Fig. 5 and Fig. 6) in the same dewar and cooled down same rate as the baseline test.

Figure 5: ODU HWR being loaded in the dewar at JLab.

Figure 6: Loading cavity in the dewar. The QWR at TRIUMF.

Testing

The tests followed the procedure below.

- Cooldown – For the first test we cooled down the cavity as fast as we could to minimize trapped flux. The cooldown rate was about 1 hour from room temperature to 4.3 K as shown in the Fig. 7.
- System calibration – Mainly cable calibration when the helium bath temperature and cavity temperature reached 4.3 K.
- Multipacting processing – Multipacting was observed mostly at first frequency 325 MHz. Usually multipacting did not appear again or minimal at next frequency.
- Fine Q measurement at 4.3 K.
- Slow cooldown to 2 K and Q measurement at a fixed series of field levels during cooldown.
- Fine step Q measurement at 2 K.
- Further cooldown to 1.5 K.
- Cable calibration – A full cable calibration was performed at the end of the test to verify the cable attenuation has been consistent during test. A typical change was 0.1-0.2 dB.
- Warm up – The dewar was warmed up to 4.3 K and the test was repeated at the next frequency.
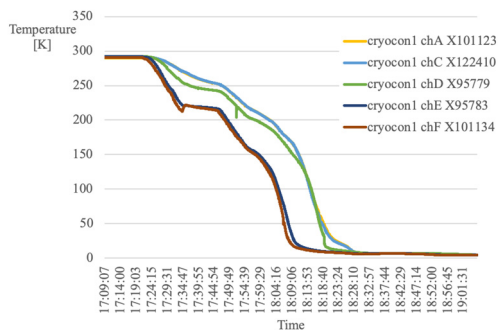
Figure 7: Cavity temperature change during cooldown from room temperature to 4.3 K.

Analysis Procedure

After performing the Q measurement, the data are processed as follows:

- Extract average Rs from geometric factor for series of fixed Bp. The average surface resistance R_s can be calculated from each series of Q measurement.

$$G = \frac{\int_V dV |\mathbf{H}|^2}{\int_S dS |\mathbf{H}|^2} \qquad \overline{R}_s(H) = G / Q(H)$$

- The average R_s points are fitted to the following formula with 3 fitting parameters A, D and R_{res}.

$$\overline{R}_s = \frac{A}{T} \exp\left(-\frac{D}{T}\right) + R_{res}$$

The formula has a temperature dependent part which is based on BCS theory and a temperature independent part called residual resistance.

- From the fit we obtain $A(B_p)$, $D(B_p)$, $R_{res}(B_p)$ at a given frequency. This allows us to obtain the average $\overline{R}_s$ for any fixed bath temperature T is found.
- Extract real $R_s(B_p)$ for any fixed bath T [7].
- Repeat for each frequency.
- Find frequency dependence of all parameters: $A(B_p, \omega)$, $D(B_p, \omega)$, $R_{res}(B_p, \omega)$.
- Correction for bath temperature vs internal surface temperature if needed.

TEST RESULTS AND ANALYSIS

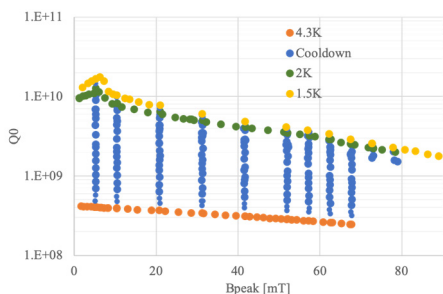A typical Q measurement data obtained from the process described above is shown in Fig. 8.

Figure 8: An example of Q measurement on ODU HWR. Test after 6 hour bake of 1302 MHz.

Average R_s is expressed as a function of temperature T. These fitted functions are shown in Fig. 9 for baseline tests of ODU HWR.
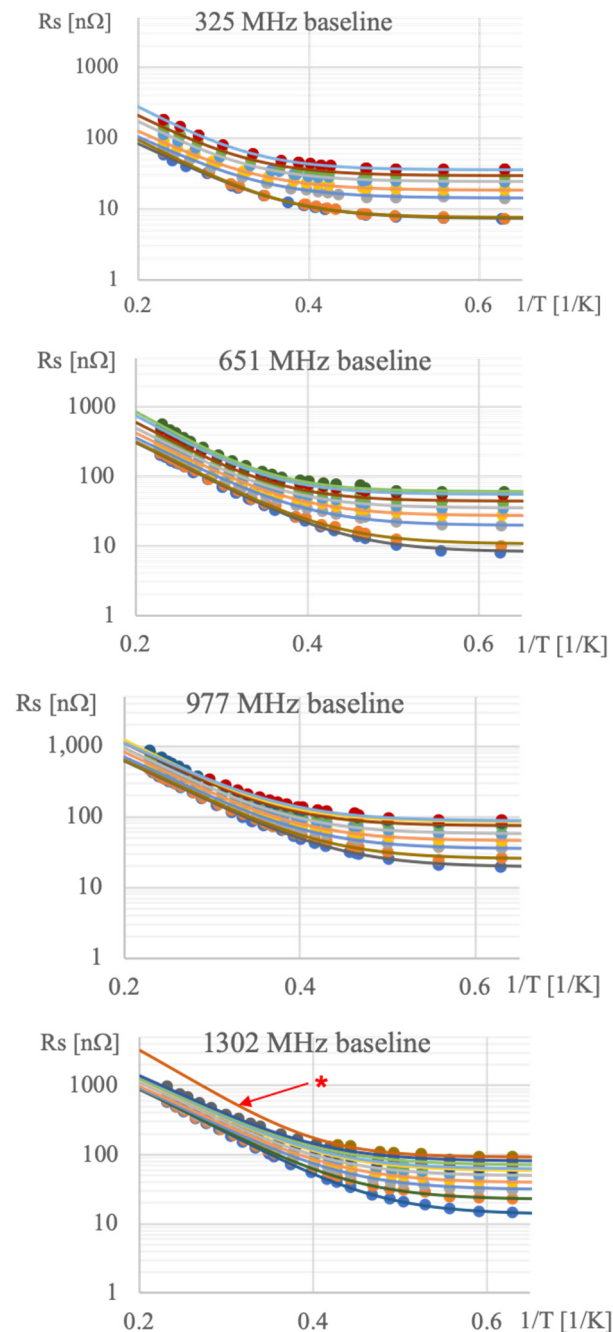

Figure 9: Average R_s as a function of T at different field levels at TEM frequencies baseline. The solid lines are fitted line based on measured data points. The asterisk * shows unrealistic fit R_s due to insufficient amount of data.

The analysis of TRIUMF QWR data followed the similar procedure. The example plots of QWR 217 MHz data is shown in Fig. 10.
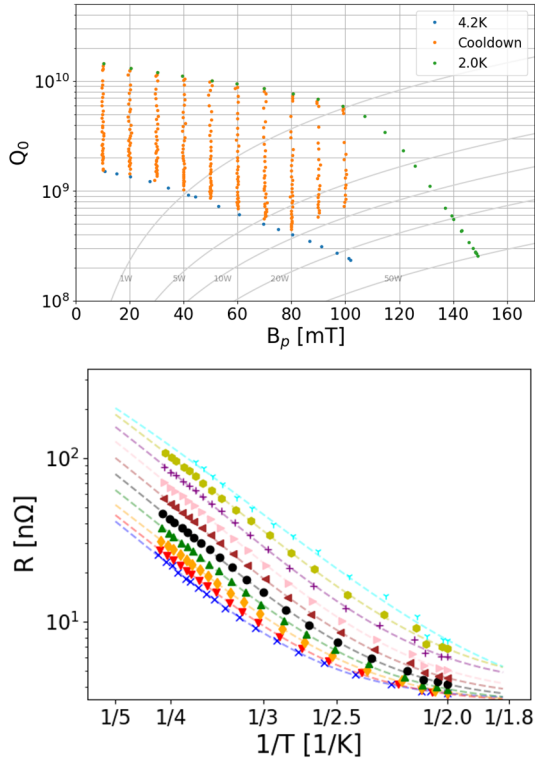
Figure 10: TRIUMF 217 MHz QWR data. The Q measurements (top) and the extracted average R_s (bottom).

During the process of data fitting, it was noted that the insufficient amount data leads to a grossly deviated outlier. Those outliers are excluded in next analysis step.

Real R_s can be calculated from the average R_s using newly developed procedure [7].

The distribution of the surface magnetic field in a particular mode in a cavity can be represented by the function $a(h)$ which is the fraction of the total cavity area where the surface magnetic field is less than $h H_p$ where H_p is the peak surface magnetic field. For half-wave cavities the function $a(h)$ is the same for all the TEM modes and can be obtained analytically.

If the average surface resistance $\overline{R_s}(H)$ can be expanded in a sum of powers (not necessarily integer) of the magnetic field, then the real surface resistance $R_s(H)$ will have the same power expansion but with the coefficient of each power term modified by the parameters $\beta(\alpha)$.

$$\overline{R}_s(H) = R_0 \sum_{\alpha_i} r_{\alpha_i} \left(\frac{H}{H_0} \right)^{\alpha_i}$$

$$R_s(H) = R_0 \sum_{\alpha_i} r_{\alpha_i} \beta(\alpha_i) \left(\frac{H}{H_0} \right)^{\alpha_i}$$

$$\beta(\alpha) = \frac{2 \int_0^1 dh \, h[1 - a(h)]}{(2+\alpha) \int_0^1 dh \, h^{1+\alpha}[1 - a(h)]}$$

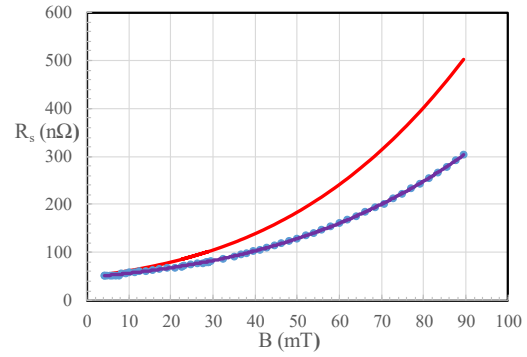An example of real R_s is plotted in Fig. 11 and Fig. 12.

Figure 11: Real R_s extracted from ODU HWR 325 MHz baseline test at 4.3K. The red line is calculated real R_s.
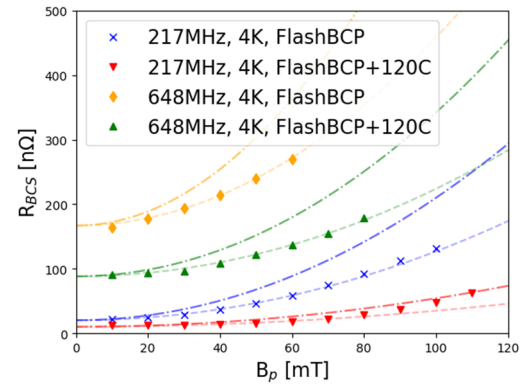

Figure 12: Real R_s extracted from data. Solid markers are extracted R_s from geometric factor, dotted lines are fitted line and dashed dot line is real R_s. Data are from QWR measurement by TRIUMF.

From the fit, one can find field dependence of 3 fit parameters; A, D, and Rres and examine the field and frequency dependence.

Parameter A

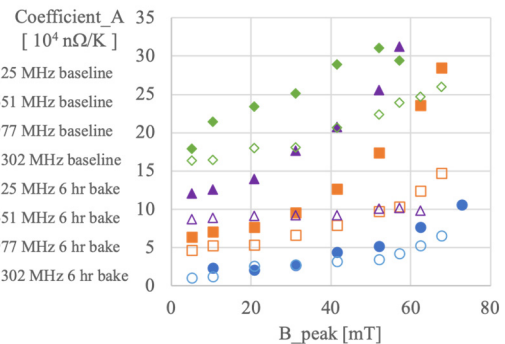The field dependence of parameter A is found shown Fig. 13 for ODU HWR case.

Figure 13: Field dependence of parameter A.

Figure 14 is the field dependence plot of parameter A of TRIUMF QWR.
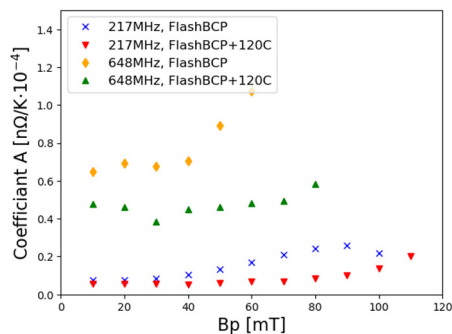
Figure 14: TRIUMF QWR result. Baseline is after bulk BCP, heat treatment 800 C 6 hours and flash BCP. Low temp baking at 120C was for 48 hours.

In both cases of HWR and QWR, the parameter A exhibits a field dependence. It seems the parameter A has a linear dependence on the field. However, a linear fit equation is purposely not shown because it seems premature to quantify the dependence with the data including localized defect.

Once all frequency data are collected, the frequency dependence can be found. Figure 15 shows the frequency dependence of parameter A at very low field.
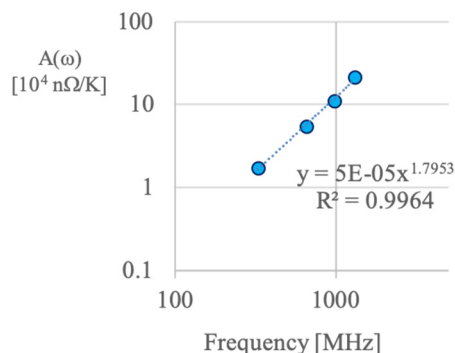

Figure 15: Frequency dependence of parameter A at 3 mT on ODU HWR.

At low field, the parameter has power dependence over frequency, $\omega^{\sim 1.8}$. According to the BCS theory, which is determined by the factors such as temperature (T), angular frequency (ω), and material properties of penetration depth (λ), energy gap (Δ), coherence length which expressed as following formula.

$$R_{BCS} = \frac{\mu_0^2 \omega^2 \lambda^3 \sigma_n \Delta}{k_B T} \ln\left[\frac{C_1 k_B T}{\hbar \omega}\right] \exp\left[-\frac{\Delta}{k_B T}\right]$$

Here μ_0, k_B, $\hbar$ are permeability in free space, the Boltzmann constant, and the Planck constant respectively.

Often, it is said that the R_{BCS} is dependent on ω^2. But when the material parameters of niobium were substituted in the formula or in codes used to calculate the surface resistance, the frequency dependence is closer to $\omega^{\sim 1.8}$ due to the $\ln[1/\omega]$ factor.

The frequency dependence at higher fields appears to be different, as shown in Fig. 16.

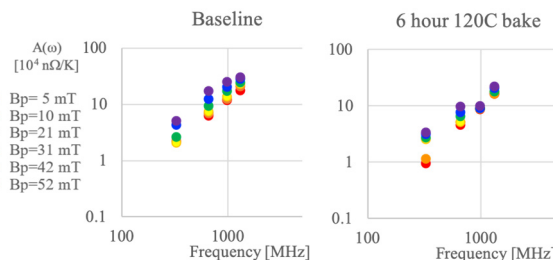
Figure 16: Frequency dependence of parameter A.

At the baseline test, the frequency dependence has the same trend over the different field levels. However, after 6 hour bake, the field dependence decreases as the field increases.

Parameter D

The ODU HWR did not show any particular trend as shown in Fig. 17. The average over all data points is 19.14 K.
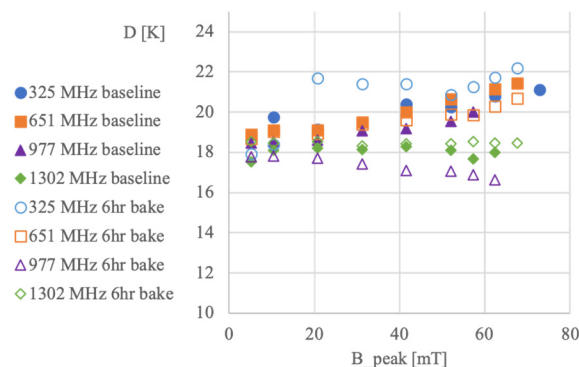

Figure 17: Field dependence of parameter D of ODU HWR.

TRIUMF QWR results show a weak field dependence of the same parameter (see Fig. 18).
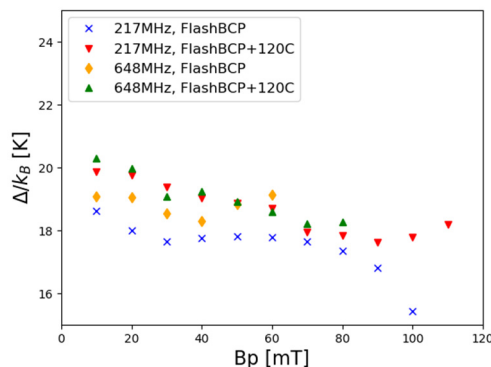

Figure 18: Field dependence of parameter D for QWR.

Parameter R_{res}

The temperature independent parameter R_{res} are plotted as a function of field in Fig. 19. Throughout different frequencies and treatment, R_{res} shows its dependence of the field.
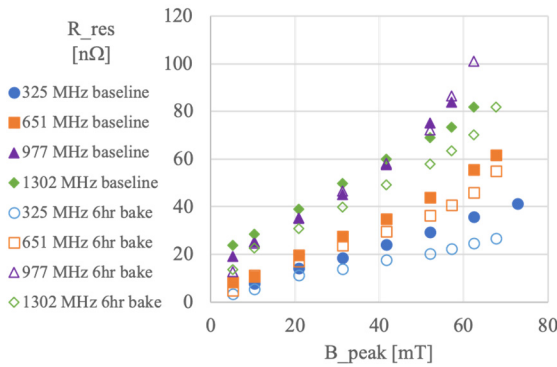
Figure 19: Field dependence of parameter R_{res} for ODU HWR.

TRIUMF QWR results also shows the dependence of R_{res} on the field as in Fig. 20. Interestingly, their slopes are composite with initial zero slope at lower field and constant slope at higher field.
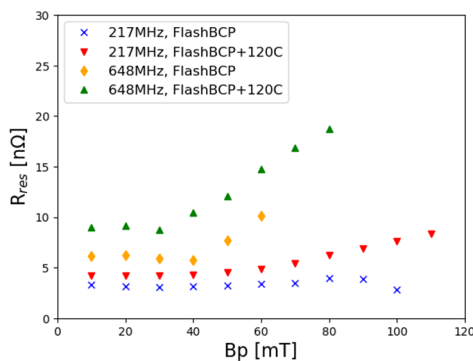

Figure 20: Field dependence of R_{res} for TRIUMF QWR.

The effect of baking is opposite for HWR and QWR. For HWR the baking made R_{res} decrease but it made R_{res} of QWR increase. The difference between two cases is mainly baking time. HWR was baked for 6 hours and QWR was baked for 48 hours.

In terms of frequency dependence of R_{res}, it shows the dependence of $\omega^{-1.5}$ at very low field (see Fig. 21).
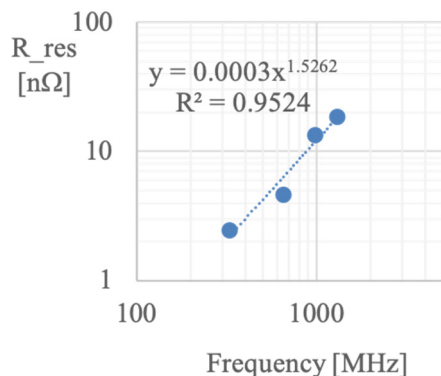

Figure 21: Frequency dependence of parameter R_{res} at 3 mT.

It appears the frequency dependence (slope) decreases as the field increases (see Fig. 22). Trapped vortices are known to be a source of residual resistance and frequency dependant. Effect of trapped vortices in this results is subject of further experiment.
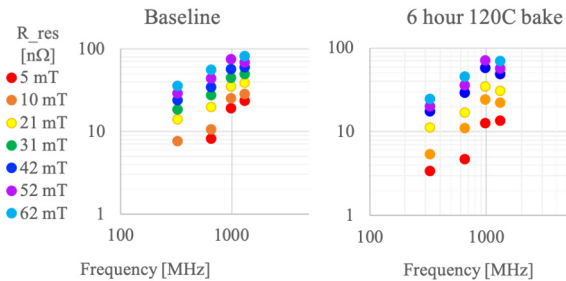

Figure 22: Frequency dependence of parameter R_{res}.

LESSONS LEARNED

We found both HWR at ODU and QWR at TRIUMF were not able to reach the maximum field at 4.3K. As one can see in the Fig. 8 and Fig. 10, the quench field is increasing as temperature decreases which tells the limited field at the higher temperature was due to insufficient cooling. To improve the cooling, ODU is planning to increase the center conductor diameter for the new cavity. TRIUMF changed the position of the cavity (place cavity in vertical instead of horizontal) in the dewar and saw the improvement already. The Q measurement shows a Q switch at low field around 5 mT. The temperature monitoring during the cryogenic test indicates a defect potentially at the top end of the center conductor. These localized defects make the interpretation of the data analysis difficult since the analysis is based on the assumption of uniform surface property. It is crucial for this study that the cavity should be free of defects, multipacting or field emission.

FUTURE EXPLORATION

In short term, ODU will repeat the experiments with second HWR cavity and is in process of building third cavity. TRIUMF is starting test with HWR cavity soon and their QWR is ready for nitrogen infusion study.

The main goal of the long-term program is to understand the origin of nonlinear loss mechanisms and how to improve the cavity performance based on the insight obtained from the analysis. The following cavity treatments are subject to the initial test campaign.

- Low temperature baking – As shown in the test results of ODU and TRIUMF, further investigation will be helpful to see how baking time affects the surface resistance in the frequency range of interest. If it does, the field and frequency dependence will provide insight behind the mechanism and how to optimize it. ODU will continue baking study incrementally increasing baking time up to 96 hours.
- Nitrogen doping/infusion

- Flux expulsion study
- Electropolishing
- High temperature heat treatment

In fact, the above surface treatments have been extensively studied with elliptical cavities of 1.3 – 1.5 GHz. The treatment optimized for a particular design and frequency may not be the best solution for low frequency and complex structured cavities like HWR, QWR, spoke cavities, or crabbing cavities. We expect these studies will find the best option for these cavities.

Another long-term goal is to explore new srf materials such as Nb_3Sn coating, NbTi, and MgB_2.

CONCLUSIONS

Studies on surface resistance with multimode cavities show great potential that will help us to understand all the contributions to the power dissipation in superconductors at rf frequencies of interest. As we observed from the preliminary results and their analyses, the methodology can extract the field and frequency dependence of each surface treatment. The findings can be applied to the surface treatment for a specific frequency.

One should keep in mind the underlying assumption is that the surface has uniform rf properties.

Surface field distribution is almost identical for all TEM modes of HWR and QWR, much better than elliptical cavities but not exactly so. This is a source of errors in addition to the measurement errors. The errors will have to be vigorously analysed.

Wide range of data collection is absolutely necessary for correct analysis. Since we do not yet have full control of all parameters, results contain randomness and no final conclusion should be drawn based on limited set of data.

Reproducibility is utmost important to establish trustworthy analysis results. It is advisable to repeat the same experiment preferably in different institutions.

We would like to emphasize that these results are preliminary and that no definite conclusion can yet be drawn. We are in the initial stage of an extensive campaign that will benefit from a collaboration between laboratories interested in improving the performance of superconducting cavities, especially those of complicated shape, operating cw, and at low frequencies.

ACKNOWLEDGEMENT

REFERENCES

[1] J. Bardeen, L. N. Cooper, and J. R. Schrieffer, "Theory of Superconductivity," *Phys. Rev.*, vol. 108, p. 1175, Dec. 1957.

[2] A. Gurevich, "Superconducting Radio-Frequency Fundamentals for Particle Accelerators," *Rev. Accel. Sci. Tech*, pp. 119-146, 2012.

[3] H. Park, S. U. De Silva, and J. R. Delayen, "Superconducting Cavity for the Measurements of Frequency, Temperature, RF field dependence of the Surface Resistance", in *Proc. SRF'15*, Whistler, BC, Canada, Sep. 2015, pp. 70-73.

[4] Z. Yao *et al.,* "Designing of Multi-Frequency Coaxial Test Resonators," in *Proc. SRF'17*, Lanzhou, China, Jul. 2017, pp. 531-534.

[5] P. Kolb, R. E. Laxdal, and Z. Yao, "Low Frequency, Low β Cavity Performance Improvement Studies," presented at SRF'19, Dresden, Germany, Jul. 2019, paper TUP046, this conference.

[6] https://link.springer.com/content/pdf/10.100 7%2FBF01394760.pdf

[7] J. R. Delayen, H. Park, S. U. De Silva, G. Ciovati, and Z. Li, "Determination of the magnetic field dependence of the surface resistance of superconductors from cavity tests," *Phys. Rev. Accel. Beams*, vol. 21, p. 122001, Dec. 2018.